Human Mutation (In Press; uncorrected) www.wiley.com/humanmutation

MEAN AGE-OF-ONSET OF FAMILIAL ALZHEIMER DISEASE CAUSED BY PRESENILIN MUTATIONS CORRELATES WITH BOTH INCREASED Aβ42 AND DECREASED Aβ40

Samir Kumar-Singh [1,2]*, Jessie Theuns [1,2]*, Bianca Van Broeck [1,2], Daniel Pirici [1,2], Krist'l Vennekens [1,2], Ellen Corsmit [1,2], Marc Cruts [1,2], Bart Dermaut [1,2], Rong Wang [3], Christine Van Broeckhoven [1,2]

[1] Neurodegenerative Brain Diseases Group, Department of Molecular Genetics, Flanders Interuniversity Institute of Biotechnology and [2] Laboratory of Neurogenetics, Institute Born-Bunge, University of Antwerp, Antwerpen, Belgium [3] Department of Human Genetics, Mount Sinai School of Medicine, New York, USA. * Joint first authors

Address correspondence to Dr. Samir Kumar-Singh, MD, PhD; or Prof. Christine Van Broeckhoven, PhD, DSc. VIB8 - Department of Molecular Genetics, Neurodegenerative Brain Diseases Group. University of Antwerp, Universiteitsplein 1, B-2610 Antwerp, Belgium. Tel: +32 3 2651002; Fax: +32 3 2651012; Email: samir.kumarsingh@ua.ac.be or christine.vanbroeckhoven@ua.ac.be

The varied ways in which mutations in presenilins (PSEN1 and PSEN2) affect amyloid β precursor protein (APP) processing in causing early-onset familial Alzheimer disease (FAD) are complex and not yet properly understood. Nonetheless, one useful diagnostic marker is an increased ratio of Aβ42 to Aβ40 (Aβ42/Aβ40) in patients' brain and biological fluids as well as in transgenic mice and cells. We studied Aβ and APP processing for a set of nine clinical PSEN mutations on a novel and highly reproducible ELISA-based *in vitro* method and also sought correlation with brain Aβ analyzed by image densitometry and mass spectrometry. All mutations significantly increased Aβ42/Aβ40 *in vitro* by significantly decreasing Aβ40 with accumulation of APP C-terminal fragments, a sign of decreased PSEN activity. Only for half of the mutations tested, a significant increase in absolute levels of Aβ42 was observed. We also showed that age-of-onset of PSEN1-linked FAD correlated inversely with Aβ42/Aβ40 (r = - 0.89; *P* = 0.001) and absolute levels of Aβ42 (r = - 0.83; *P* = 0.006), but directly with Aβ40 levels (r = 0.69; *P* = 0.035). These changes also partly correlated with brain Aβ42 and Aβ40 levels. Together our data suggested that Aβ40 might be protective by perhaps sequestering the more toxic Aβ42 and facilitating its clearance. Also, the *in vitro* method we described here is a valid tool for assaying the pathogenic potential of clinical PSEN mutations in a molecular diagnostic setting.

INTRODUCTION

Presenilin 1 (PSEN1, OMIM 104311) and presenilin 2 (PSEN2, OMIM 600759) are multimeric proteins and essential components of the γ-secretase complex that degrades a number of type I proteins including the amyloid precursor protein (APP, OMIM 104760) and Notch (Marjaux et al., 2004). Mutations in the genes encoding presenilins (*PSEN1* and *PSEN2*) cause aggressive forms of early-onset familial Alzheimer disease (AD; FAD, OMIM 104300) (Cruts and Van Broeckhoven, 1998). Different mutations in *PSEN* are being identified due to the growing application of molecular diagnostics (more than 150 are already known; annotated on

www.molgen.ua.ac.be/ADMutations), however, no standardized assay or tool is yet available to predict their pathogenic potential.

Studies in human brain, cerebrospinal fluid (CSF) and plasma, as well as in transgenic animals and cellular systems modeling FAD mutations, all showed that the Aβ42/Aβ40 ratio is consistently elevated (Scheuner et al., 1996; Mann et al., 1996a; Borchelt et al., 1996; Duff et al., 1996; Citron et al., 1997; Xia et al., 1997; Tomita et al., 1997; Mehta et al., 1998; Murayama et al., 1999). This led to the premise that FAD mutations cause AD by *Aβ42*-driven 'gain of function', which is also the primary tenet of the 'amyloid cascade hypothesis' (Hardy and Selkoe, 2002). In brain, Aβ exists both as an insoluble deposited form as well as a soluble pool, and recent data suggested that the latter might be more pathogenic (Wang et al., 1999; McLean et al., 1999). Similarly, an intracellular Aβ42 pool has also been observed but does not contribute to the secreted Aβ pool (Skovronsky et al., 1998). Many recent lines of evidence also suggested that clinical *PSEN* mutations, in addition to increasing Aβ42, could also cause PSEN loss of function. Firstly, genetic studies have suggested that decreased PSEN expression increases AD risk (Theuns et al., 2003). Secondly, while wild type PSEN could substitute for a homologous protein in *C. elegans*, PSEN FAD mutants were less efficient (Levitan et al., 1996; Baumeister et al., 1997). Thirdly, in cellular systems, 6 different PSEN mutations were shown to significantly reduce Notch cleavage (Song et al., 1999). Fourthly, a reduced APP processing was also observed in PSEN-mediated γ-secretase site processing of APP (Moehlmann et al., 2002; Chen et al., 2002; Walker et al., 2005; Wiley et al., 2005). Whether clinical PSEN mutations also cause 'loss of function' became even more important in light of recent evidence that loss of presenilin in mice (Psen) causes neurodegeneration implying that in addition to Aβ42-driven gain of aberrant function, loss of PSEN function might also contribute to neurodegeneration (Saura et al., 2004).

We had two objectives in this study. One, we wanted to develop a highly reproducible *in vitro* technique for comparing the ratio of Aβ42 to Aβ40 (Aβ42/Aβ40) between different *PSEN* mutations, but also evaluating individual contributions of Aβ42 and Aβ40 to this ratio, which had been difficult due to uncontrolled transfections and cell growth patterns. Two, we wanted to test whether *PSEN* mutations caused a clinically relevant increase in Aβ42 or a decrease in Aβ40, and whether these changes corroborated with brain depositions. Utilizing a controlled, chromosomally-stable and highly reproducible *in vitro* technique, we showed here that the Aβ40 levels were dramatically decreased for all nine FAD-linked PSEN mutations studied, while the Aβ42 levels were significantly increased for only half of these mutations. We also showed that not only an increase in Aβ42 levels or in the Aβ42/Aβ40 ratio, but also a drop in Aβ40 levels significantly correlated with age-of-onset of clinical manifestations of FAD-linked PSEN1 mutations.

MATERIALS AND METHODS

Mutations and patients

We studied eight *PSEN1* mutations dispersed all over the protein that cause FAD at ages-of-onset classified as very early (<40 years), early (40-50 years), or mid-life (50-65 years) (Table). A further selection criteria was based on either in-house availability of neuropathological data (see below), or re-identification of these mutations in our molecular diagnostics unit or in ongoing population-based genetic studies. In addition, we also studied the best-documented, *PSEN2* N141I (Volga German) mutation (see Table). Mean ages-of-onset were taken from the self-curated AD mutation database (www.molgen.ua.ac.be/ADMutations). For age-of-onset of AD in the general population, a mean age of 75.3 years ascertained in 504 patients was utilized (Engelborghs et al., 2003) in whom the prevalence of PSEN or APP mutations is < 0.05% (Van Broeckhoven *et al.*, unpublished data). Brains

from 6 PSEN1 mutation carriers (A79V, n = 1 patient; I143T, n = 6 patients; C263F, n = 3 patients; L282V, n = 2 patients; G384A, n = 6 patients; Δ9, n = 1 patient) were available. The mean disease durations from onset to death when listed on the mutation database were utilized, which closely matched the mean disease durations in our families. For A79V, mean disease duration of 10 years (Cruts et al., 1998; Finckh et al., 2000) and for C263F, a duration of 7.7 years were utilized (unpublished data). In addition, 8 sporadic AD with mean age-of-onset of 73.8 years and mean disease duration of 7.4 years were included as controls.

Constructs

Human APP695 cDNA carrying the APP/Sw mutation (Table) was subcloned in the pcDNA-5 Flp-In recombinase vector system (Invitrogen, Groningen, The Netherlands). The full-length coding part of *PSEN1* cDNA was available (De Jonghe et al., 1999), and the coding part of *PSEN2* cDNA (van de Craen et al., 1999) was recloned into the *Kpn*I and *BamH*I sites of pcDNA3. *PSEN1* and *PSEN2* mutations were introduced using the QuickChange site-directed mutagenesis system (Stratagene, La Jolla, CA, USA) and confirmed by sequencing (primer sequences are available on request).

Generation of *APP* and *PSEN* double stable cell lines

Human embryonic kidney 293 Flp-In (HEK293 Flp-In, Invitrogen) cells were maintained in DMEM containing 10% fetal calf serum (FCS, Invitrogen) and 2mM L-glutamine (Invitrogen). Cells were first transfected with APP/Sw (Murayama et al., 1999) utilizing Fugene (Roche, New Jersey, NJ, USA). HEK293 Flp-In cells containing a "single" transposed copy of APP/Sw at the defined Flp recombinase target site were selected in the presence of 400 μg/ml hygromycin (Duchefa, Haarlem, The Netherlands). Cells were further transfected with *PSEN* mutants in pcDNA3 and genomically stable *PSEN* integrations were selected in the presence of 750 μg/ml neomycin G418 (Promega, Leiden, The Netherlands). Three independent polyclonal stables were made for each *PSEN* construct and studied in duplicate.

Real-time RT-PCR

To study the *PSEN* transcripts in transfected cells, mRNA was prepared using the magnetic beads-based Chemagic mRNA Direct Kit (Chemagen, Baesweiler, Gemany). cDNA was synthesized with random primers using the Superscript III First-Strand Synthesis System for RT-PCR (Invitrogen). Primers and Taqman® MGB probes for real-time PCR analysis were designed using PrimerExpress software (Applied Biosystems, Werrington, UK). cDNA was quantified on an ABI7900 HT instrument using the universal amplification protocol (Applied Biosystems). Two housekeeping genes, *B2M* (*β-2-microglobulin*) and *UBC* (*ubiquitin C*) were utilized for normalization (sequences of primers and probes are available on request).

Western blotting and metabolic labeling

Cell lysates for PSEN western blotting were prepared in RIPA buffer with protease inhibitors, as described previously (Kumar-Singh et al., 2002). Proteins (20 μg), measured on a bicinchoninic acid (BCA) colorimetric assay (Perbio Science N.V., Aalst, Belgium), were separated on a 4-12% Bis-Tris Nupage gel (Invitrogen) and electroblotted onto a polyvinylidene difluoride membrane (Hybond P®; Amersham Biosciences, Aylesbury, UK). Membranes were immunoblotted with either SB128 (1:2000) rabbit antisera against N-terminal fragment of PSEN1 (De Jonghe et al., 1999) or B24.2 (1:10000) affinity purified rabbit antisera to the C-terminal fragment of PSEN2. Immunodetection was done with secondary antibody and ECL plus chemiluminescent detection system (Amersham Biosciences) with bands quantified on Kodak Imaging Station 440 (Eastman Kodak, Rochester, NY, USA). Quantitative data were normalized to the signal obtained for β actin (clone AC-15; Sigma, Missouri, USA).

Aβ secreted in the supernatant of transfected cells was studied by isotopic immunoprecipitation studies as described previously (De Jonghe et al., 2001; Wiltfang et al., 2001). Briefly, cells were labeled with 100 µCi [35S]methionine (ICN, Irvine, CA, USA) in methionine-free medium for 4 h, and conditioned medium (1 ml) collected and immunoprecipitated with 4.5 µl of polyclonal anti-Aβ anibody B106.1 and 25 µl of protein G-Sepharose (Amersham Biosciences). Proteins were separated on 8 M urea Bicine/Tris SDS PAGE (Wiltfang et al., 2001), and the intensity of the radioactive bands was quantified using a phosphoimager (Molecular Dynamics, Sunnyvale, CA, USA) and the ImageQuant software (De Jonghe et al., 2001). APP C-terminal fragment (CTF), α and β stubs, were immunoprecipitated with polyclonal antibody B63.1 and immune complexes recovered with protein G-Sepharose and resolved on a 10% NuPAGE gel and MES buffer (Invitrogen).

Aβ1-40 and Aβ1-42 ELISA

Subconfluent cell layers were conditioned for 24 h in highly enriched Optimem (Invitrogen) in absence of FCS as it interferes with the Aβ ELISA. Aβ42 and Aβ40 concentrations were measured in 2- to 10-fold diluted conditioned media by a sandwich-type enzyme-linked immunosorbent assay (ELISA), using the Innotest β-amyloid 1-42 (Innogenetics, Zwijndrecht, Belgium) and human β-amyloid 1-40 ELISA (Biosource Europe, Nivelles, Belgium). Recombinant human Aβ (Calbiochem, La Jolla, CA, USA) and empty pcDNA3 vector expressing APP/Sw alone were used as controls.

Development of a normalization technique for cellular viability

To correct Aβ levels in the supernatants for variations in the number of viable cells between culture dishes or between the different PSEN mutants studied, we developed a normalization technique based on assessment of constitutively secreted cytokines from the cell supernatants thus avoiding errors in accurately collecting cells for lysate-based normalization. Also, because measurements are made after FCS withdrawal that causes some cells to have extended growth latencies, measurement of cytokines offers an estimation of functionally viable cells. For this, non-transfected HEK293 cells as well as cells transfected with mutant and wild type PSEN were initially assayed for transforming growth factor β1 (TGFB1; R&D), fibroblast growth factor (FGF; Perbio), hepatocyte growth factor (HGF; Perbio), and heparin-binding EGF-like growth factor (HB-EGF; Perbio). Correlations were made between the PSEN allele and the number of cells seeded. TGFB1 was the most robust cytokine secreted and remained unaffected in presence of different PSEN mutations. TGFB1 normalization was further compared with normalizations based on other methods, i.e., BCA-based total protein measurements, GAPDH-ELISA (Active Motif, Carlsbad, CA, USA), actin western blotting, and trypan-blue exclusion cell count independently by 2 investigators (Figure 1).

Brain Aβ40 and Aβ42 image and mass spectrometric analysis

Aβ densitometry was performed on formalin-fixed paraffin-embedded tissue from the frontal and temporal cortex of 6 PSEN1 mutation carriers and 8 sporadic AD patients. For one PSEN1 L282V carrier, the temporal cortical region was not available. Serial 5 µm thick sections were sliced and consecutive sections were stained with Aβ40 (R209) or Aβ42 (JRF/cAb42/12) (Kumar-Singh et al., 2000) using 3',3' diaminobenzidine tetrahydrochloride (DAB; Roche) as detailed elsewhere (Kumar-Singh et al., 2005). Three such series were made for each tissue block and images analyzed as described previously (Kumar-Singh et al., 2005). Briefly, sections were imaged with an Axioskop 50 microscope (Carl Zeiss NV, Zaventem, Belgium) equipped with a CCD Olympus DP camera and software (Soft Imaging System Gmbh, Münster, Germany). The entire sections were scanned and a grid superimposed with orthogonal X and Y steps of 2 mm. Ten images were grabbed by a 4x objective (1.93 mm^2) at coordinates intersecting the cortex for each

section. Plaque area proportion and integrated optical density of Aβ40- and Aβ42-containing plaques were determined by the NIH Scion Image analysis program (Scion Corporation, Frederick, MD, USA) on an 8-bits gray scale with an internal calibrator. Amyloid load (levels) was calculated by summing integrated optical densities of the thresholded pixels for all plaques measured. All sections were stained and images analyzed together with the same settings and calibration values.

For mass spectrometric Aβ analysis, we utilized freshly frozen tissue with a relatively short autopsy period from patients from two extended PSEN1 early-onset families (I143T and G384A; n = 3 patients each) as well as from 8 sporadic AD brains. Temporal cortical regions were dissected from frozen tissue blocks on which a prior Aβ immunohistochemistry had shown abundant Aβ depositions. Tissue was homogenized in formic acid to extract soluble and deposited protein. Aβ peptides were isolated by immunoprecipitation using monoclonal antibody 4G8 (Wang et al., 1996; Kumar-Singh et al., 2000) and analyzed by a matrix-assisted laser-desorption/ionization-time-of-flight (MALDI-TOF) mass spectrometer (Voyager-DE STR BioSpectrometry Workstation, PE/PerSeptive Biosystem; Boston, MA, USA), as described previously (Wang et al., 1996; Kumar-Singh et al., 2000).

Statistical analysis

Aβ40 and Aβ42 are expressed as mean (pg/ml) ± SEM. A one-way analysis of variance (ANOVA) was performed to compare between average levels of Aβ40, Aβ42 or Aβ42/Aβ40 secreted from PSEN1 wild type and mutants; *a priori* contrast method further tested Aβ levels and ratio between PSEN1 wild type and different mutants. A *t* test was also used to compare the Aβ levels and ratio produced by PSEN wild type and mutant transfectants. Levene's test was used to test that the variances in Aβ levels and ratio were equal in both the *t* test and ANOVA comparisons. Similarly, histochemical and mass spectrometric Aβ40, Aβ42 or Aβ42/Aβ40 were analyzed by *t* test and multiple comparisons adjusted according to Bonferroni's method. Linear regression analysis with strength of relationship measured by Pearson correlation coefficients was utilized to correlate Aβ levels and age-of-onset of dementia. For this, Aβ42 and Aβ40 measurements were $\log_e$ transformed based on plotting and residual studies. All statistical analyses were performed with SPSS 12.0 (SPSS Inc., Chicago, IL, USA).

RESULTS

Clinical *PSEN* mutations led to variable degrees of APP-CTF accumulation and consistently decreased Aβ40

We studied 8 PSEN1 mutations (A79V, I143T, A231V, L262F, C263F, L282V, G384A, Δ9) that cause FAD with varying ages-of-onset as well as the best-documented PSEN2 mutation (N141I; Volga-German). Because endogenous Aβ is at the limit of detection, we first transfected HEK293 Flp-In cells with APP/Sw (Citron et al., 1992; Murayama et al., 1999). However, the uniqueness of this system is that all cells integrate a single copy of APP/Sw at a chromosomally defined site with APP expression consistent between different cell lines (Figure 2 B, upper panel). We further stably transfected these cells with the different mutant and wild type *PSEN1* cDNA constructs and studied whether the double-stable cells uniformly expressed *PSEN* and if it was processed normally. A real-time PCR transcript analysis showed that the *PSEN* expression from stably transfected clones, normalized to either of the two house keeping genes, *B2M* and *UBC*, was uniform between *PSEN* mutants and wild type, with a ≈10 fold higher expression of the transcript compared to cells with an empty vector (data not shown). On the protein level, all *PSEN* mutants generated normal steady state levels of full-length (FL) protein and N-terminal fragments (NTF) compared to the wild type (Figure 2 A) and compared to the empty vector, an expected ≈2 fold higher NTF was observed for *PSEN* mutants and wild type. For PSEN1 Δ9, an increase in PSEN expression was

exclusively seen for the FL band with downregulation of endogenous PSEN, as has been observed earlier (Thinakaran et al., 1997).

We further studied APP-CTF from which Aβ is generated by PSEN-mediated γ-secretase activity. Accumulation of APP-CTF is thus a sign of reduced PSEN activity. Immunoprecipitation-gel experiments showed that APP-CTF accumulated to different extents in all PSEN mutants studied compared to PSEN wild type (Figure 2 B). Accumulation of APP-CTF was most appreciable for PSEN1 A79V, A231V, C263F, L282V, and to some extent, for PSEN2 N141I. Furthermore, immunoprecipitation experiments showed that Aβ40 was reduced for all PSEN mutations while an appreciable Aβ42 band was only visible for 4 PSEN mutations: PSEN1 G384A, Δ9, I143T, and PSEN2 N141I. For the others, although Aβ42 could be viewed under high contrast, these bands could not be reliably quantified. Only in PSEN1 I143T, a parallel increase in shorter Aβ peptides (i.e. Aβ1-39) was observed.

Cell-secreted Aβ42/Aβ40, Aβ40 and Aβ42 correlated with age-of-onset of dementia

To quantitatively study Aβ40 and Aβ42, we utilized an Aβ40- and Aβ42-specific sandwich ELISA. A statistically significant difference of means was observed in Aβ42/Aβ40 ratio between PSEN1 mutants and wild type (0.34 ± 0.305 versus 0.07 ± 0.032, respectively; ANOVA, regression SS = 4.549, df = 8; residual SS = 0.370 df = 45; F = 69.161, $P < 0.001$). *A priori* contrast test showed that the differences were mainly contributed by three mutations: G384A, Δ9, and I143T (P for all < 0.001). A *t* statistics, however, showed that Aβ42/Aβ40 was significantly higher for all PSEN1 and PSEN2 mutations compared to the wild type ($P \leq 0.01$), in agreement with previous studies (Scheuner et al., 1996; Borchelt et al., 1996; Duff et al., 1996; Citron et al., 1997; Tomita et al., 1997; Mehta et al., 1998; Murayama et al., 1999; Walker et al., 2005) (Figure 3 A).

To quantify the absolute levels of Aβ40 and Aβ42, we developed a functional method that allowed to assess the precise amounts of absolute Aβ40 and Aβ42 (see *Methods*). Using this system, we showed that absolute levels of Aβ42 were significantly higher in PSEN1 mutation carriers compared to wild type (12.2 ± 10.29 versus 6.6 ± 4.02, respectively; ANOVA, regression SS = 3231.257, df = 8; residual SS = 1999.477, df = 45; F = 9.09, $P < 0.001$), and contrast ANOVA found significant differences again for G384A, Δ9, and I143T ($P \leq 0.002$). A *t* test for PSEN2 N141I also showed a significant increase in absolute Aβ42 levels ($P = 0.008$). These were precisely the same mutations for which Aβ42 bands were observed on the immunoprecipitation-gel experiments. Interestingly, absolute levels of Aβ40 substantially dropped for PSEN1 mutations compared to wild type (94.4 ± 17.02 versus 41.7 ± 15.01, respectively; ANOVA, regression SS = 18528.877, df = 8; residual SS = 8309.813, df = 45; F = 12.5, $P < 0.001$), and contrast test identified the Aβ40 drop to be a consistent feature for *all* PSEN1 mutations compared to the wild type ($P < 0.001$). A similar drop in Aβ40 was also present in PSEN2 N141I compared to its wild type (*t* test, $P = 0.003$).

Absolute levels of Aβ42 and Aβ40 as well as the Aβ42/Aβ40 ratio were correlated with age-of-onset of clinical PSEN1 mutations (Figure 3). We showed that age-of-onset of dementia correlated inversely with the Aβ42/Aβ40 ratio (Pearson's coefficient correlation, r = - 0.89, $P = 0.001$) and absolute levels of Aβ42 (r = - 0.83, $P = 0.006$). In addition, we showed a significant direct correlation between age-of-onset of AD and absolute levels of Aβ40 (r = 0.69, $P = 0.035$).

Brain Aβ42 deposits correlated with cell-secreted Aβ

To study whether cell-secreted Aβ correlated with brain Aβ deposition, we assessed Aβ40 or Aβ42 immunohistochemical loads in temporal and frontal cortices from 6 PSEN1 mutation(s) carriers (A79V, n = 1; I143T, n = 6; C263F, n = 3; L282V, n = 2; G384A, n = 1; and Δ9, n = 6) and sporadic AD patients (n = 8). Both PSEN1 and sporadic AD

brains deposited robust Aβ42 and Aβ40. A statistically significant difference between PSEN1 and sporadic AD was observed for average *area* proportion of the tissue occupied by Aβ42 immunostaining (P = 0.005), but not by Aβ40 (P = 0.060). However, because Aβ40 is predominant in dense-core plaques in contrast to the Aβ42 predominance in the faintly immunoreactive diffuse plaques, we further studied the integrated optical densities (area * average densities) representing brain Aβ levels (Figure 4 A, B). This was possible as the brains had comparable post mortem delay; were similarly processed for embedding; and the sections were stained and analyzed in the same setting. Both Aβ42 and Aβ40 brain levels were significantly higher in PSEN1 mutation carriers compared to sporadic AD patients ($P \leq 0.005$). This difference was mainly contributed by G384A, I143T, and Δ9 (for individual P values, see Figure 4 A). However, some of the sporadic AD brains deposited more Aβ42 and Aβ40 than some PSEN1 mutation carriers, a notable example being A79V patient. A significant correlation was also observed between brain and cell-secreted Aβ42 (r = 0.83; n = 7, P = 0.020), however, no such correlation was observed between brain and cell-secreted Aβ40 (r = - 0.55; P = 0.195). In contrast, a high degree of correlation was present between Aβ40 and Aβ42 brain levels (r = 0.79, n = 27 patients, $P < 0.001$). No significant correlations were observed between brain Aβ40, Aβ42, or Aβ42/Aβ40 and mean age-of-onset ($P \geq 0.07$). Similarly, mean disease duration also did not correlate significantly with brain Aβ40 levels or Aβ42/Aβ40 ratio ($r^2 \geq$ - 0.49; P ≥ 0.06), but correlated with a borderline significance with brain Aβ42 levels (r^2 = -0.76; P = 0.045).

Brain Aβ40 and Aβ42 levels measured by image analysis were compared with Aβ immunoprecipitation and MALDI-TOF mass spectrometry (IP/MS) for 8 sporadic AD patients and 3 patients each for the PSEN1 I143T and G384A. Unlike image analysis, Aβ IP/MS provided a more accurate Aβ42/Aβ40 assessment and also differentiated between Aβ with different N-termini (i.e., starting at D1, E11, L17, etc). This was important as ELISA only measured "full-length" Aβ1-40 and Aβ1-42. Full-length Aβ1-42 and Aβ1-40 emerged as two of the most robust Aβ measurements in brain. For some I143T and G384A brains, Aβ11-42 emerged to be a major peak (Figure 4 C), but in general, a good correlation was observed between full-length Aβ and their N-truncated variants (Pearson's coefficient correlation, r ≥ 0.95, n =14, $P < 0.001$). Similarly, Aβ42 measured by image analysis correlated strongly with IP/MS Aβ42 measurements (r = 0.84, $P < 0.001$), and moderately with Aβ40 loads measured by the two methods (r = 0.68, P = 0.008).

DISCUSSION

Mutations in *PSEN* are the most important cause of early-onset, aggressive forms of autosomal dominant FAD. The number of known *PSEN* mutations is constantly growing due to the utilization of DNA diagnostics in genetic counseling for AD. Unfortunately, however, genetic information to definitively prove the disease-causing potential of these novel mutations is frequently lacking, necessitating the use of biological assays to confirm their pathological character. One of the most important effects noticed for all FAD mutations is an aberrant APP processing resulting in an elevated Aβ42/Aβ40 ratio in brain, CSF, and plasma (Scheuner et al., 1996; Mann et al., 1996a; Borchelt et al., 1996; Duff et al., 1996; Citron et al., 1997; Xia et al., 1997; Tomita et al., 1997). This property has been utilized for successfully developing numerous transgenic cell culture assays that have the primary advantage of determining the disease-causing potential of FAD mutations independent of other heritable or environmental factors. These studies have confirmed the proof of principle of an elevated *in vitro* Aβ42/Aβ40 for *PSEN* FAD mutations (Mehta et al., 1998; Murayama et al., 1999; De Jonghe et al., 2001; Walker et al., 2005), but not for benign polymorphisms (Dermaut et al., 1999). Moreover, despite occasional observations of trends of correlation between Aβ42/Aβ40 ratio

and the mean age-of-onset of PSEN-linked FAD, no statistical significance was observed (Murayama et al., 1999; De Jonghe et al., 2001; Walker et al., 2005; Mehta et al., 1998). The unreliability and non-reproducibility of the data has, to some extent, limited the use of genetic testing in a clinical setting (Croes et al., 2000).

One of the frequent problems encountered in the *in vitro* Aβ experiments is an uncontrolled PSEN/APP transgenic expression and normalization based on western blotting that in our hands was the least reliable of all methods tested. While Aβ42/Aβ40 ratio could still be calculated, these limitations had precluded an accurate quantification of the individual Aβ40 or Aβ42 levels. We developed a well-controlled and highly reproducible method that not only differentiated pathogenic mutations from wild type, but the sensitivity offered by this method also allowed predictions of human ages-of-onset in PSEN-linked FAD. The advantages offered by the present method are the following: firstly, the γ-secretase complex is currently known to constitute at least 4 proteins, including PSEN (Marjaux et al., 2004); thus a human-derived cellular assay offers a more "physiological" γ-secretase complex formation than that provided by animal-derived cell lines with heterologous human PSEN expression (Murayama et al., 1999; Walker et al., 2005). Secondly, a uniform, chromosomally stable PSEN expression along with the presence of endogenous wild type *PSEN* more closely mimics human disease where *PSEN* mutations affect only one allele. This system, thus, allows the possible "dominant negative effect" of a *PSEN1* mutation to be studied as well (Wolfe et al., 1999), which was not possible with studies involving Psen double knock-out mouse embryonic fibroblasts (DKO-MEF) (Walker et al., 2005). The Psen DKO-MEF system has been earlier proposed to have the advantage of studying biological functions of different PSEN mutations without the interference of endogenous Psen proteins (Annaert and De Strooper, 2002). However, there are some concerns that overexpressing human *PSEN* in Psen DKO-MEF is not entirely stable due to the initial absence of Psen protein and destabilization of the γ-secretase machinery. Thirdly, in the current system, the cells integrate a "single copy of *APP/Sw*" at a chromosomally defined site that provides a uniform APP production against which the effect of PSEN mutations can be studied, however, prevents overwhelming pathways for Aβ40 or Aβ42 secretion. Fourthly, to correct Aβ levels in the supernatants for variations in the number of viable cells between culture dishes, or between different PSEN mutations, a "functional cytokine (TGFB1) assay" allows a more accurate normalization of secreted Aβ. And lastly, "internal Aβ calibrators" further reduce the experiment-to-experiment variation occurring with non-precise amounts of synthetic Aβ peptides used as Aβ standards in each kit/experiment.

Using this *in vitro* technique and a well-represented set of *PSEN* mutations, we showed that the Aβ42/Aβ40 ratio was significantly elevated for all mutations and strongly correlated with age-of-onset of AD. A correlation coefficient of 0.89 (r^2 = 0.79), suggests that 79% of the variance in age-of-onset of familial *PSEN1* or sporadic AD (wild type and mutant *PSEN1* alleles) is explained by the Aβ42/Aβ40 ratio, or a factor closely linked to it (i.e., CTF or AICD, see later). The rest is due to other genetic variants or environmental factors. Importantly, for the first time we showed that not only an increased Aβ42 (r^2 = 0.69), but also a drop in Aβ40 (r^2 = 0.48) correlated significantly with mean age-of-onset of clinical PSEN1 AD. Very recently, a similar correlation of age-of-onset with Aβ42/Aβ40 ratio was reported (r^2 = 0.96) with an entirely different set of *PSEN1* mutations than those reported here, however, perhaps due to the difficulties in measuring Aβ42 and Aβ40, a similar correlation was not found for Aβ42 and none at all for Aβ40 (r^2 = 0.56 and 0.03, respectively; Duering et al., 2005).

We next studied whether *in vitro* Aβ ELISA data correlated with the deposited brain Aβ load studied by image and mass spectrometric analysis. As shown earlier (Mann et al., 1996a), *PSEN1* mutation carriers had a higher mean brain

Aβ level compared to sporadic patients, although some sporadic AD patients had more Aβ42 deposition than select PSEN-linked FAD patients, i.e., A79V. We also showed that cell-secreted Aβ42 correlated well with brain Aβ42 deposition, although no such correlation was observed for Aβ40 and is consistent with earlier observations (Murayama et al., 1999; Mann et al., 2001). A recent study of CSF Aβ40 levels could not even differentiate AD from non-demented controls, while Aβ42 levels and Aβ42/Aβ40 ratio were able to do so (Lewczuk et al., 2004). Moreover, in contrast to cell-secreted Aβ, neither brain Aβ42 nor Aβ40 correlated significantly with mean age-of-onset. When similar correlations were sought with the mean duration of clinical illness, a borderline significant correlation was observed for brain Aβ42 levels, but none at all for Aβ40. There are several explanations for this. First, immunohistochemical analysis also identifies a huge burden of N-truncated Aβ42 plaques typically present in "non-pathogenic" diffuse plaques (Dickson, 1997; Iwatsubo et al., 1996), while an ELISA, such as the one described here, measures only the "pathogenic", full-length Aβ1-42. Secondly, after the appearance of clinical symptoms, the progression of disease is rather fast. For instance, even sporadic AD patients despite having a much later age-of-onset, show a disease duration of 6-10 years, which is similar to that observed in many *PSEN1* mutation carriers. For instance, the average Aβ42 brain deposition in sporadic AD patients in this series exceeded those observed in A79V brain and fits well with a shorter disease duration (7.2 years) than that observed for A79V (10 years). And lastly, the lack of a significant correlation of age-of-onset with brain Aβ42 still looked more like a matter of statistical power due to a limited number of brains/mutations that could be analyzed in any single setting, which in turn further emphasizes the importance of an *in vitro* diagnostic assay. However, with Aβ40 the situation was more complex as its deposition closely followed that of Aβ42. For instance, G384A led to one of the most significant *in vitro* decrease in Aβ40; however, brains of these patients still deposited Aβ40 substantially. These observations were not due to the higher age groups or overrepresentations of ApoE4, factors that have earlier been shown to influence deposition of Aβ40 more than that of Aβ42 (Iwatsubo et al., 1995; Mann et al., 1996a; Mann et al., 1997). Instead, these data fit well with Aβ42 seeding Aβ40 deposition as suggested by the amyloid cascade hypothesis. For instance, G384A also drastically increases Aβ42 *in vitro* as well as in brain, and it is likely that these provide nidi for further Aβ40 deposition to form dense-core plaques commonly observed in G384A brains (Mann et al., 1996b). These data fit well with recent data on transgenic mice where Aβ40 has been shown to be important for dense-core plaque formation (Kumar-Singh et al., 2005; Miao et al., 2005), but not without an Aβ42 seed (Herzig et al., 2004; McGowan et al., 2005). Thus, while an increased brain Aβ42 secretion and its subsequent deposition would coerce Aβ40 deposition despite its decreased levels caused by FAD mutations, only a critical drop in Aβ40 (≈ 80%) would parallel its decreased deposition in brain as has been observed for APP T714I (Kumar-Singh et al., 2000).

And lastly, we showed here that an *in vitro* drop in Aβ40, despite correlating less well with age-of-onset compared to Aβ42 was one of the most consistent features noticed for all *PSEN1* FAD mutations studied here. While only half of these mutations significantly altered Aβ42 levels on ELISA that were also obvious on immunoprecipitation-gel experiments. Loss of Aβ40 or other signs of decreased APP processing have also been confirmed for clinical *PSEN2* mutations (Walker et al., 2005); as well as for clinical *APP* γ-secretase site mutations (Ancolio et al., 1999; Kumar-Singh et al., 2000; De Jonghe et al., 2001; Wiley et al., 2005). It remains possible that the decreased Aβ40 underlies some other APP cleavage defect, for instance, loss of APP-intracellular domain (AICD) or accumulation of CTF that could instead cause toxicity (Wiley et al., 2005 and references therein). However, transgenic mice studies have supported a protective role for Aβ40, as different mice lines with no difference in Aβ42 levels deposit amyloid plaques only if Aβ40

levels are below a critical threshold (Mucke et al., 2000).

To conclude, we showed here for the first time on a novel *in vitro* AD diagnostic method, a significant and strong correlation between age-of-onset of AD and increased Aβ42/Aβ40 and Aβ42 levels, and decreased Aβ40 levels. In fact, a consistent decrease in Aβ40 was observed for all FAD-*PSEN* mutations studied here and was most drastic (and accompanied by APP-CTF accumulation) for those FAD-*PSEN* mutants that had an earlier age-of-onset. Whether a significant direct association of age-of-onset of *PSEN* FAD is due to a drop in Aβ40 levels *per se* or due to some other defect closely linked to APP processing is open for future investigation.

Note added as proof: While this study was under submission, a report published by the group of Bart De Strooper has shown a similar loss of function for FAD-*PSEN1* alleles (Bentahir et al., 2006).

Acknowledgements: We thank Dr. B. De Strooper for B106.1 and B63.1 antisera; Drs. W. Annaert, P Mehta, and M. Mercken for B24.2, R209, and JRF/cAb42/12 antibodies, respectively; and the Antwerp brain bank of Institute Born-Bunge as well as the Amsterdam brain bank for providing brains. This study was funded by the Special Research Fund of the University of Antwerp, the Fund for Scientific Research Flanders (FWO-F), the Interuniversity Attraction Poles (IUAP) program P5/19 of the Belgian Science Policy Office (BELSPO), the International Alzheimer Research Foundation (IARF) Belgium, EU contract LSHM-CT-2003-503330 (APOPIS). Mass spectrometry was supported by NIH grant CA088325. JT and MC are postdoctoral fellows of the FWO-F.

Databases: Gene sequences: NCBI entrez nucleotide database: http://www.ncbi.nlm.nih.gov/entrez/query.fcgi?db=Nucleotide;

Protein sequences: NCBI entrez protein database: http://www.ncbi.nlm.nih.gov/entrez/query.fcgi?db=Protein;

OMIM: http://www.ncbi.nlm.nih.gov/entrez/query.fcgi?db=OMIM;

AD mutation database**:** http://www.molgen.ua.ac.be/ADMutation

References

Ancolio K, Dumanchin C, Barelli H, Warter JM, Brice A, Campion D, Frebourg T, Checler F. 1999. Unusual phenotypic alteration of beta amyloid precursor protein (APP) maturation by a new Val-715 -> Met APP-770 mutation responsible for probable early-onset Alzheimer's disease. Proc Natl Acad Sci U S A 96:4119-4124.

Annaert W, De Strooper B. 2002. A cell biological perspective on Alzheimer's disease. Annu Rev Cell Dev Biol 18:25-51.

Baumeister R, Leimer U, Zweckbronner I, Jakubek C, Grunberg J, Haass C. 1997. Human presenilin-1, but not familial Alzheimer's disease (FAD) mutants, facilitate *Caenorhabditis elegans* Notch signalling independently of proteolytic processing. Genes and Function 1:149-159.

Bentahir M, Nyabi O, Verhamme J, Tolia A, Horre K, Wiltfang J, Esselmann H, De Strooper B. 2006. Presenilin clinical mutations can affect gamma-secretase activity by different mechanisms. J Neurochem 96:732-742.

Borchelt DR, Thinakaran G, Eckman CB, Lee MK, Davenport F, Ratovitsky T, Prada CM, Kim G, Seekins S, Yager D, Slunt HH, Wang R, Seeger M, Levey AI, Gandy SE, Copeland NG, Jenkins NA, Price DL, Younkin SG, Sisodia SS. 1996. Familial Alzheimer's disease-linked presenilin 1 variants elevate Abeta1-42/1-40 ratio in vitro and in vivo. Neuron 17:1005-1013.

Chen F, Gu Y, Hasegawa H, Ruan X, Arawaka S, Fraser P, Westaway D, Mount H, George-Hyslop P. 2002. Presenilin 1 mutations activate gamma 42-secretase but reciprocally inhibit epsilon-secretase cleavage of amyloid precursor protein (APP) and S3-cleavage of notch. J Biol Chem 277:36521-36526.

Citron M, Oltersdorf T, Haass C, McConlogue L, Hung AY, Seubert P, Vigo-Pelfrey C, Lieberburg I, Selkoe DJ. 1992. Mutation of the b-amyloid precursor protein in familial Alzheimer's disease increases b-protein production. Nature 360:672-674.

Citron M, Westaway D, Xia W, Carlson G, Diehl T, Levesque G, Johnson WK, Lee M, Seubert P, Davis A, Kholodenko D, Motter R, Sherrington R, Perry B, Yao H, Strome R, Lieberburg I, Rommens J, Kim S, Schenk D, Fraser P, St George-Hyslop P, Selkoe DJ. 1997. Mutant presenilins of Alzheimer's disease increase production of 42-residue amyloid beta-protein in both transfected cells and transgenic mice [see comments]. Nat Med 3:67-72.

Croes EA, Dermaut B, Der Cammen TJ, Van Broeckhoven C, van Duijn CM. 2000. Genetic testing should not be advocated as a diagnostic tool in familial forms of dementia. Am J Hum Genet 67:1033-1035.

Cruts M, Van Broeckhoven C. 1998. Presenilin mutations in Alzheimer's disease. Hum Mutat 11:183-190.

Cruts M, van Duijn CM, Backhovens H, Van den Broeck M, Wehnert A, Serneels S, Sherrington R, Hutton M, Hardy J, St George-Hyslop P, Hofman A, Van Broeckhoven C. 1998. Estimation of the genetic contribution of presenilin-1 and -2 mutations in a population-based study of presenile Alzheimer disease. Hum Mol Genet 7:43-51.

De Jonghe C, Cruts M, Rogaeva EA, Tysoe C, Singleton A, Vanderstichele H, Meschino W, Dermaut B, Vanderhoeven I, Backhovens H, Vanmechelen E, Morris CM, Hardy J, Rubinsztein DC, St George-Hyslop P, Van Broeckhoven C. 1999. Aberrant splicing in the presenilin-1 intron 4 mutation causes presenile Alzheimer's disease by increased Abeta42 secretion. Hum Mol Genet 8:1529-1540.

De Jonghe C, Esselens C, Kumar-Singh S, Craessaerts K, Serneels S, Checler F, Annaert W, Van Broeckhoven C, De Strooper B. 2001. Pathogenic APP mutations near the gamma-secretase cleavage site differentially affect Abeta secretion and APP C-terminal fragment stability. Hum Molec Genet 10:1665-1671.

Dermaut B, Cruts M, Slooter AJ, Van Gestel S, De Jonghe C, Vanderstichele H, Vanmechelen E, Breteler MM, Hofman A, van Duijn CM, Van Broeckhoven C. 1999. The Glu318Gly substitution in presenilin 1 is not causally related to Alzheimer disease. Am J Hum Genet 64:290-292.

Dickson DW. 1997. The pathogenesis of senile plaques. J Neuropathol Exp Neurol 56:321-339.

Duering M, Grimm MO, Grimm HS, Schroder J, Hartmann T. 2005. Mean age of onset in familial Alzheimer's disease is determined by amyloid beta 42. Neurobiol Aging 26:785-788.

Duff K, Eckman C, Zehr C, Yu X, Prada CM, Perez-tur J, Hutton M, Buee L, Harigaya Y, Yager D, Morgan D, Gordon MN, Holcomb L, Refolo L, Zenk B, Hardy J, Younkin S. 1996. Increased amyloid-beta42(43) in brains of mice expressing mutant presenilin 1. Nature 383:710-713.

Engelborghs S, Dermaut B, Goeman J, Saerens J, Marien P, Pickut BA, Van den BM, Serneels S, Cruts M, Van Broeckhoven C, De Deyn PP. 2003. Prospective Belgian study of neurodegenerative and vascular dementia: APOE genotype effects. J Neurol Neurosurg Psychiatry 74:1148-1151.

Finckh U, Muller-Thomsen T, Mann U, Eggers C, Marksteiner J, Meins W, Binetti G, Alberici A, Hock C, Nitsch RM, Gal A. 2000. High prevalence of pathogenic mutations in patients with early-onset dementia detected by sequence analyses of four different genes. Am J Hum Genet 66:110-117.

Hardy J, Selkoe DJ. 2002. The amyloid hypothesis of Alzheimer's disease: progress and problems on the road to therapeutics. Science 297:353-356.

Herzig MC, Winkler DT, Burgermeister P, Pfeifer M, Kohler E, Schmidt SD, Danner S, Abramowski D, Sturchler-Pierrat C, Burki K, van Duinen SG, Maat-Schieman MLC, Staufenbiel M, Mathews PM, Jucker M. 2004. A beta is targeted to the vasculature in a mouse model of hereditary cerebral hemorrhage with amyloidosis. Nature Neuroscience 7:954-960.

Iwatsubo T, Mann DM, Odaka A, Suzuki N, Ihara Y. 1995. Amyloid beta protein (Aß) deposition: Aß42(43) precedes Aß40 in Down syndrome. Ann Neurol 37:294-299.

Iwatsubo T, Saido TC, Mann DM, Lee VM, Trojanowski JQ. 1996. Full-length amyloid-beta (1-42(43)) and amino-terminally modified and truncated amyloid-beta 42(43) deposit in diffuse plaques. Am J Pathol 149:1823-1830.

Kumar-Singh S, De Jonghe C, Cruts M, Kleinert R, Wang R, Mercken M, De Strooper B, Vanderstichele H, Lofgren A, Vanderhoeven I, Backhovens H, Vanmechelen E, Kroisel PM, Van Broeckhoven C. 2000. Nonfibrillar diffuse amyloid deposition due to a gamma(42)-secretase site mutation points to an essential role for N-truncated abeta(42) in Alzheimer's disease. Hum Molec Genet 9:2589-2598.

Kumar-Singh S, Julliams A, Nuyens D, Labeur C, Vennekens K, Serneels S, Van Osta P, Geerts H, De Strooper B, Van Broeckhoven C. 2002. In vitro studies of Flemish, Dutch, and wild type Amyloid ß (Aß) provide evidence for a two-stage Aß neurotoxicity. Neurobiol Disease 11:300-310.

Kumar-Singh S, Pirici D, McGowan E, Serneels S, Ceuterick C, Hardy J, Duff K, Dickson D, Van Broeckhoven C. 2005. Dense core plaques in Tg2576 and PSAPP mouse models of Alzheimer's disease are centered on vessel walls. Am J Pathol 167:527-543.

Levitan D, Doyle TG, Brousseau D, Lee MK, Thinakaran G, Slunt HH, Sisodia SS, Greenwald I. 1996. Assessment of normal and mutant human presenilin function in *Caenorhabditis elegans*. Proc Natl Acad Sci U S A 93:14940-14944.

Lewczuk P, Esselmann H, Otto M, Maler JM, Henkel AW, Henkel MK, Eikenberg O, Antz C, Krause WR, Reulbach U, Kornhuber J, Wiltfang J. 2004. Neurochemical diagnosis of Alzheimer's dementia by CSF Abeta42, Abeta42/Abeta40 ratio and total tau. Neurobiol Aging 25:273-281.

Mann DM, Iwatsubo T, Cairns NJ, Lantos PL, Nochlin D, Sumi SM, Bird TD, Poorkaj P, Hardy J, Hutton M, Prihar G, Crook R, Rossor MN, Haltia M. 1996a. Amyloid b protein Ab deposition in chromosome 14-linked Alzheimer's disease: predominance of Ab42(43). Ann Neurol 40:149-156.

Mann DM, Iwatsubo T, Ihara Y, Cairns NJ, Lantos PL, Bogdanovic N, Lannfelt L, Winblad B, Maat-Schieman ML, Rossor MN. 1996b. Predominant deposition of amyloid-beta 42(43) in plaques in cases of Alzheimer's disease and hereditary cerebral hemorrhage associated with mutations in the amyloid precursor protein gene. Am J Pathol 148:1257-1266.

Mann DM, Iwatsubo T, Pickering-Brown SM, Owen F, Saido TC, Perry RH. 1997. Preferential deposition of amyloid beta protein (Abeta) in the form Abeta40 in Alzheimer's disease is associated with a gene dosage effect of the apolipoprotein E E4 allele. Neurosci Lett 221:81-84.

Mann DM, Pickering-Brown SM, Takeuchi A, Iwatsubo T. 2001. Amyloid Angiopathy and Variability in Amyloid beta Deposition Is Determined by Mutation Position in Presenilin-1-Linked Alzheimer's Disease. Am J Pathol 158:2165-2175.

Marjaux E, Hartmann D, De Strooper B. 2004. Presenilins in memory, Alzheimer's disease, and therapy. Neuron 42:189-192.

McGowan E, Pickford F, Kim J, Onstead L, Eriksen J, Yu C, Skipper L, Murphy MP, Beard J, Das P, Jansen K, Delucia M, Lin WL, Dolios G, Wang R, Eckman CB, Dickson DW, Hutton M, Hardy J, Golde T. 2005. Abeta42 is essential for parenchymal and vascular amyloid deposition in mice. Neuron 47:191-199.

McLean CA, Cherny RA, Fraser FW, Fuller SJ, Smith MJ, Beyreuther K, Bush AI, Masters CL. 1999. Soluble pool of Abeta amyloid as a determinant of severity of neurodegeneration in Alzheimer's disease. Ann Neurol 46:860-866.

Mehta ND, Refolo LM, Eckman C, Sanders S, Yager D, Perez tJ, Younkin S, Duff K, Hardy J, Hutton M. 1998. Increased Abeta42(43) from cell lines expressing presenilin 1 mutations. Ann Neurol 43:256-258.

Miao J, Xu F, Davis J, Otte-Holler I, Verbeek MM, Van Nostrand WE. 2005. Cerebral microvascular Aß protein deposition induces vascular degeneration and neuroinflammation in transgenic mice expressing human vasculotropic mutant AßPP. Am J Pathol 167:505-515.

Moehlmann T, Winkler E, Xia X, Edbauer D, Murrell J, Capell A, Kaether C, Zheng H, Ghetti B, Haass C, Steiner H. 2002. Presenilin-1 mutations of leucine 166 equally affect the generation of the Notch and APP intracellular domains independent of their effect on Abeta 42 production. Proc Natl Acad Sci U S A 99:8025-8030.

Mucke L, Masliah E, Yu GQ, Mallory M, Rockenstein EM, Tatsuno G, Hu K, Kholodenko D, Johnson-Wood K, McConlogue L. 2000. DO NOT USE High-Level Neuronal Expression of Abeta 1-42 in Wild-Type Human Amyloid Protein Precursor Transgenic Mice: Synaptotoxicity without Plaque Formation. Journal of Neuroscience 20:4050.

Murayama O, Tomita T, Nihonmatsu N, Murayama M, Sun X, Honda T, Iwatsubo T, Takashima A. 1999. Enhancement of amyloid beta 42 secretion by 28 different presenilin 1 mutations of familial Alzheimer's disease. Neurosci Lett 265:61-63.

Saura CA, Choi SY, Beglopoulos V, Malkani S, Zhang D, Shankaranarayana Rao BS, Chattarji S, Kelleher RJ, III, Kandel ER, Duff K, Kirkwood A, Shen J. 2004. Loss of presenilin function causes impairments of memory and synaptic plasticity followed by age-dependent neurodegeneration. Neuron 42:23-36.

Scheuner D, Eckman C, Jensen M, Song X, Citron M, Suzuki N, Bird TD, Hardy J, Hutton M, Kukull W, Larson E, Levy LE, Viitanen M, Peskind E, Poorkaj P, Schellenberg G, Tanzi R, Wasco W, Lannfelt L, Selkoe D, Younkin S. 1996. Secreted amyloid beta-protein similar to that in the senile plaques of Alzheimer's disease is increased in vivo by the presenilin 1 and 2 and APP mutations linked to familial Alzheimer's disease. Nat Med 2:864-870.

Skovronsky DM, Doms RW, Lee VM. 1998. Detection of a novel intraneuronal pool of insoluble amyloid beta protein that accumulates with time in culture. J Cell Biol 141:1031-1039.

Song W, Nadeau P, Yuan M, Yang X, Shen J, Yankner BA. 1999. Proteolytic release and nuclear translocation of Notch-1 are induced by presenilin-1 and impaired by pathogenic presenilin-1 mutations. Proc Natl Acad Sci U S A 96:6959-6963.

Theuns J, Remacle J, Killick R, Corsmit E, Vennekens K, Huylebroeck D, Cruts M, Van Broeckhoven C. 2003. Alzheimer-associated C allele of the promoter polymorphism -22C>T causes a critical neuron-specific decrease of presenilin 1 expression. Hum Mol Genet 12:869-877.

Thinakaran G, Harris CL, Ratovitski T, Davenport F, Slunt HH, Price D, Borchelt DR, Sisodia SS. 1997. Evidence that levels of presenilins (PS1 and PS2) are coordinately regulated by competition for limiting cellular factors. J Biol Chem 272:28415-28422.

Tomita T, Maruyama K, Saido TC, Kume H, Shinozaki K, Tokuhiro S, Capell A, Walter J, Grunberg J, Haass C, Iwatsubo T, Obata K. 1997. The presenilin 2 mutation (N141I) linked to familial Alzheimer disease (Volga German families) increases the secretion of amyloid beta protein ending at the 42nd (or 43rd) residue. Proc Natl Acad Sci U S A 94:2025-2030.

van de Craen M, De Jonghe C, van den Brande I, Declercq W, Van Gassen G, van Criekinge W, Vanderhoeven I, Fiers W, Van Broeckhoven C, Hendriks L, Vandenabeele P. 1999. Identification of caspases that cleave presenilin-1 and presenilin-2. Five presenilin-1 (PS1) mutations do not alter the sensitivity of PS1 to caspases. FEBS Lett 445:149-154.

Walker ES, Martinez M, Brunkan AL, Goate A. 2005. Presenilin 2 familial Alzheimer's disease mutations result in partial loss of function and dramatic changes in Abeta 42/40 ratios. J Neurochem 92:294-301.

Wang J, Dickson DW, Trojanowski JQ, Lee VM. 1999. The levels of soluble versus insoluble brain Abeta distinguish Alzheimer's disease from normal and pathologic aging. Exp Neurol 158:328-337.

Wang R, Sweeney D, Gandy SE, Sisodia SS. 1996. Use 2047-The profile of soluble amyloid ß protein in cultured cell media. Detection and quantification of amyloid ß protein and variants by immunoprecipitation-mass spectrometry. J Biol Chem 271:31894-31902.

Wiley JC, Hudson M, Kanning KC, Schecterson LC, Bothwell M. 2005. Familial Alzheimer's disease mutations inhibit gamma-secretase-mediated liberation of beta-amyloid precursor protein carboxy-terminal fragment. J Neurochem 94:1189-1201.

Wiltfang J, Esselmann H, Cupers P, Neumann M, Kretzschmar H, Beyermann M, Schleuder D, Jahn H, Ruther E, Kornhuber J, Annaert W, De Strooper B, Saftig P. 2001. Elevation of beta-amyloid peptide 2-42 in sporadic and familial Alzheimer's disease and its generation in PS1 knockout cells. J Biol Chem 276:42645-42657.

Wolfe MS, Xia W, Ostaszewski BL, Diehl TS, Kimberly WT, Selkoe DJ. 1999. Two transmembrane aspartates in presenilin-1 required for presenilin endoproteolysis and gamma-secretase activity [In Process Citation]. Nature 398:513-517.

Xia W, Zhang J, Kholodenko D, Citron M, Podlisny MB, Teplow DB, Haass C, Seubert P, Koo EH, Selkoe DJ. 1997. Enhanced production and oligomerization of the 42-residue amyloid beta-protein by Chinese hamster ovary cells stably expressing mutant presenilins. J Biol Chem 272:7977-7982.

LEGEND TO TABLE

Table: Location and the clinical information of the mutations studied.

LEGEND TO FIGURES

Figure 1: Establishment of TGFB1 normalization assay for *PSEN*/*APP* double stable cellular model. **A**: Flp-In cells were seeded in different densities in multiple wells and 2 were analyzed that appeared to have a similar confluence. The average of detailed cell-counts by two investigators and total protein measurements from the lysates correlated best with TGFB1 measurements that linearly increased over 40,000 through 120,000 per mm^2 cells seeded. Actin western analysis was less reliable. **B**: Experiments were performed separately as GAPDH lysate preparation is different from that recommended for other assays. GAPDH ELISA did not correlate well with either cell count or TGFB1 measurements. **C**: In extended series, Flp-In cells carrying different constructs were seeded in triplicate and analyzed. Well-to-well variation was appreciable for all measurements. Actin western blotting was least precise. Detailed cell counts by two investigators correlated well with the total protein measurements, but not with the TGFB1 ELISA. However, Aβ40 and Aβ42 were shown to have the least variance between the triplicates when normalized for TGFB1 compared to when normalized by other methods. Error bars represent standard deviation of 2 to 3 measurements.

Figure 2: PSEN and APP processing in a *PSEN*/*APP* double-stable cell culture model. **A**: Polyclonal stable pools overexpressed ≈2 fold PSEN1 N-terminal fragment (NTF), normalized to actin, as well as full-length (FL) protein that was absent in the empty vector. For PSEN1 Δ9, an increase was observed exclusively for the FL band as PSEN1 Δ9 protein is not endoproteolyzed. **B**: Accumulation of APP-CTFs in varying amounts in all *PSEN* mutants compared to *PSEN* wild type with an accompanying reduction in Aβ40. Aβ42 increase was most remarkable for PSEN1 G384A, Δ9, I143T, and PSEN2 N141I. For PSEN1 I143T, Aβ1-39 is also appreciable.

Figure 3: Altered Aβ processing in a cell culture model of mutant *PSEN* correlates with age-of-onset of AD. **A**: An Aβ40 and Aβ42 ELISA showed a most reliable and reproducible decrease in Aβ40 for all PSEN mutations, with only 4 PSEN mutations (PSEN1 G384A, Δ9, I143T, and PSEN2 N141I) showing a significant increase in Aβ42 secretion (measured as pg/ml). Despite this, the Aβ42/Aβ40

ratio (relative to WT; not scaled) was elevated for all. Flags represent SEM of 2 measurements from 3 independently established double-stable cell lines; *t* statistics, *, $P < 0.05$; **, $P < 0.01$; ***, $P < 0.001$. **B**: Cartoon of PSEN1 with the location of these mutations. **C**: The ages-of-onset of AD correlate significantly with Aβ42/Aβ40 ratio as well as with the Aβ42 and Aβ40 absolute amounts.

Figure 4: Brain Aβ image and mass spectrometric analysis. **A**: Image densitometry for brain Aβ42 and Aβ40 showed a large variance between different *PSEN1* mutations and also within the carriers of the same mutation as well as between different sporadic AD with similar ages-of-onset. **B**: Examples of high-levels of Aβ42 and low-levels of Aβ40-depositing PSEN1 I143T and G384A, and sporadic AD patients. Note the relative absence of Aβ40 in the same brain regions, on serial sections. **C**: Brain of the same patients studied with immunoprecipitation-mass spectrometry (IP/MS) confirmed a preponderance of Aβ42. Ins^{2+} is the internal standard used for normalization (arrows). Scale bar in *B* represents 200 μm

Table

Acronym	Gene	cDNA position [#]	Protein codon [##]	PSEN domain	Age-at-onset (years)	Disease duration (years)
A79V	*PSEN1*	c.236C>T	p.A79V	N-terminal	59.3 *	10.0 [§]
I143T	*PSEN1*	c.428T>C	p.I143T	TM-II	32.5 *	8.7 [§§]
A231V	*PSEN1*	c.692C>T	p.A231V	TM-V	58.0 *	NA
L262F	*PSEN1*	c.786G>C	p.L262F	TMVI	50.3 *	NA
C263F	*PSEN1*	c.788G>T	p.C263F	HL-VI	58.0 *	7.7 [§]
L282V	*PSEN1*	c.844C>G	p.L282V	HL-V	44.3 *	9.2 [§§]
Δ9	*PSEN1*	c.869_955del	p.(S290CT291_S319 del)	HL-VI	45.5 *	5.7 [§§]
G384A	*PSEN1*	c.1151G>C	p.G384A	TM-VII	34.9 *	7.3 [§§]
WT (Sp. AD)	*PSEN1*	–	–	–	75.3 **	7.4 [§]
Volga German	*PSEN2*	c.422A>T	p.N141I	TM-II	NA	–
APP/Sw	*APP*	c.(1953G>T;1954A>C)	p.(K670N;M671L)	–	NA	–

[#]cDNA numbering according to RefSeq number NM_000021.2 (*PSEN1*), NM_000447.1 (*PSEN2*), and NM_201413.1 (*APP*). [##]Protein numbering according to RefSeq accession number NP_000012.1 (PSEN1); NP_000438.1 (PSEN2), and NP_958816.1 (APP). Age-of-onset from AD mutation base (http://www.molgen.ua.ac.be/ADMutations) *, or from Engelborghs et al., 2003 **. Disease duration from onset to death was based on age-at-death reported on the AD mutation base [§§], or based on our families(s) [§]. NA, not available; –, not applicable.

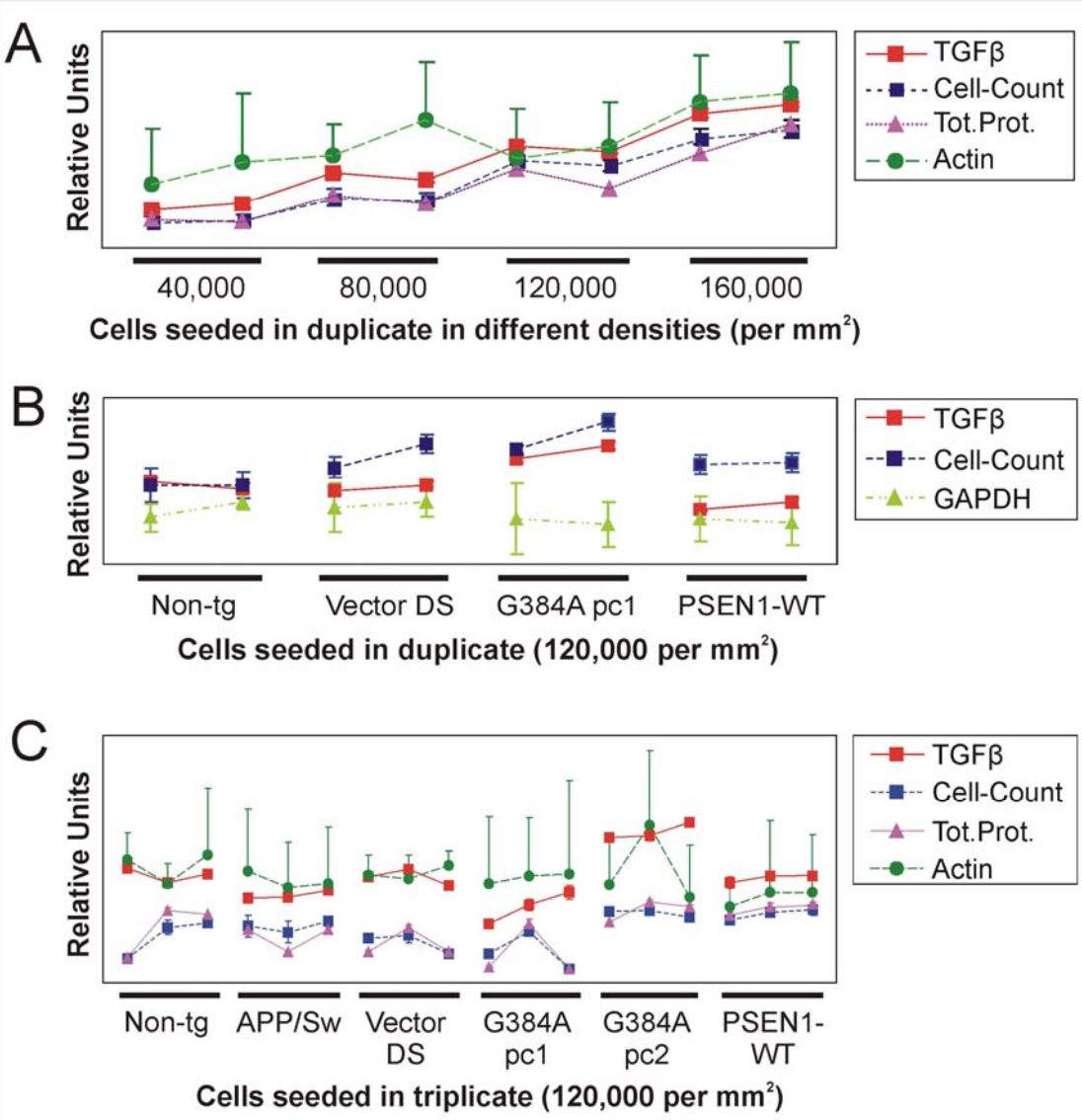
A
Relative Units
TGFβ
Cell-Count
Tot.Prot.
Actin
40,000
80,000
120,000
160,000
Cells seeded in duplicate in different densities (per mm²)
B
Relative Units
TGFβ
Cell-Count
GAPDH
Non-tg
Vector DS
G384A pc1
PSEN1-WT
Cells seeded in duplicate (120,000 per mm²)
C
Relative Units
TGFβ
Cell-Count
Tot.Prot.
Actin
Non-tg
APP/Sw
Vector DS
G384A pc1
G384A pc2
PSEN1-WT
Cells seeded in triplicate (120,000 per mm²)

Figure 1

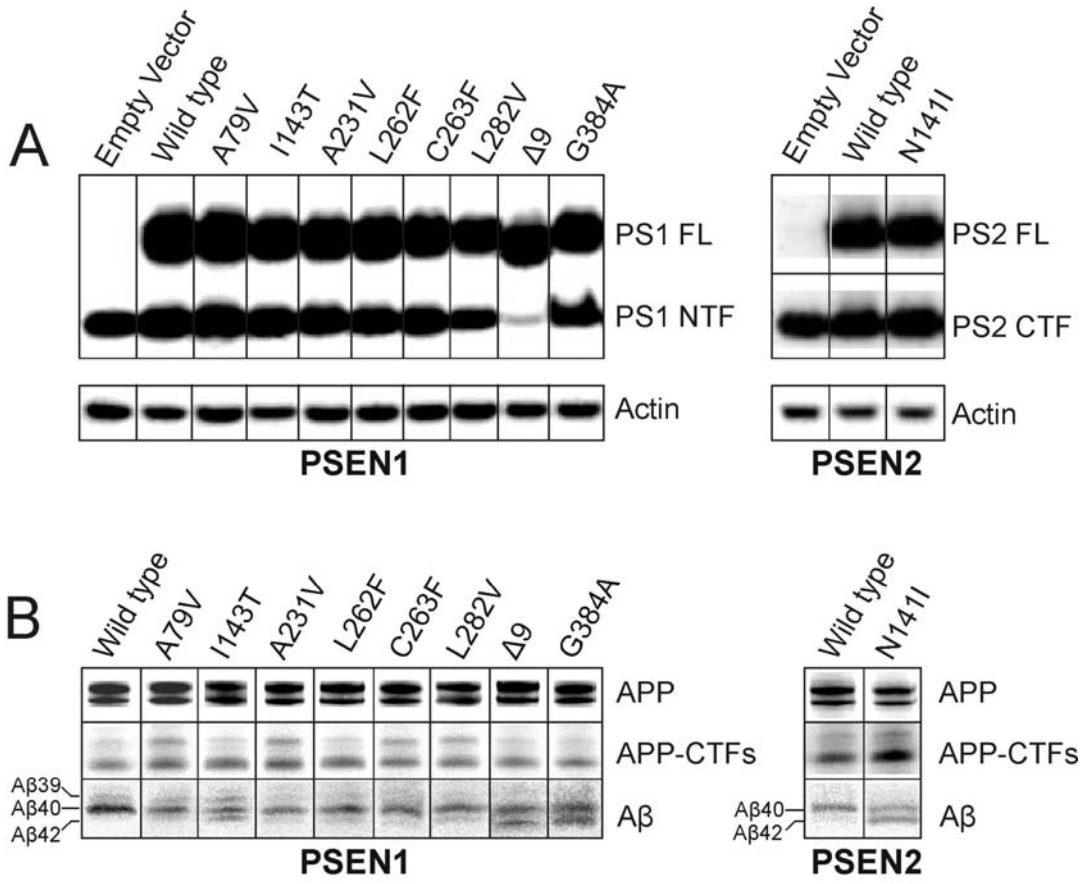
A
Empty Vector
Wild type
A79V
I143T
A231V
L262F
C263F
L282V
Δ9
G384A
PS1 FL
PS1 NTF
Actin
PSEN1
Empty Vector
Wild type
N141I
PS2 FL
PS2 CTF
Actin
PSEN2
B
Wild type
A79V
I143T
A231V
L262F
C263F
L282V
Δ9
G384A
APP
APP-CTFs
Aβ39
Aβ40
Aβ42
Aβ
PSEN1
Wild type
N141I
APP
APP-CTFs
Aβ40
Aβ42
Aβ
PSEN2

Figure 2

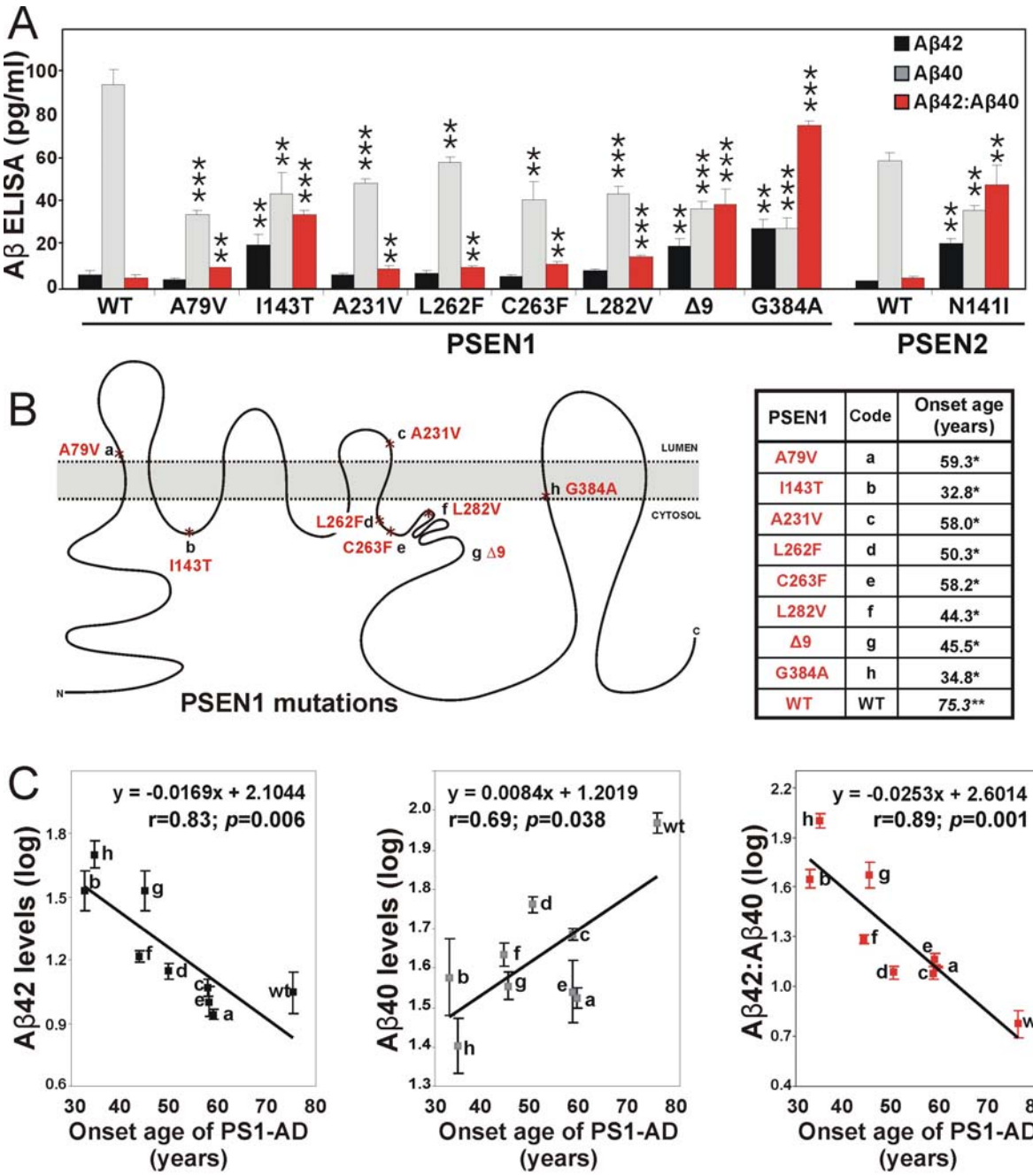

PSEN1	Code	Onset age (years)
A79V	a	59.3*
I143T	b	32.8*
A231V	c	58.0*
L262F	d	50.3*
C263F	e	58.2*
L282V	f	44.3*
Δ9	g	45.5*
G384A	h	34.8*
WT	WT	*75.3***

Figure 3

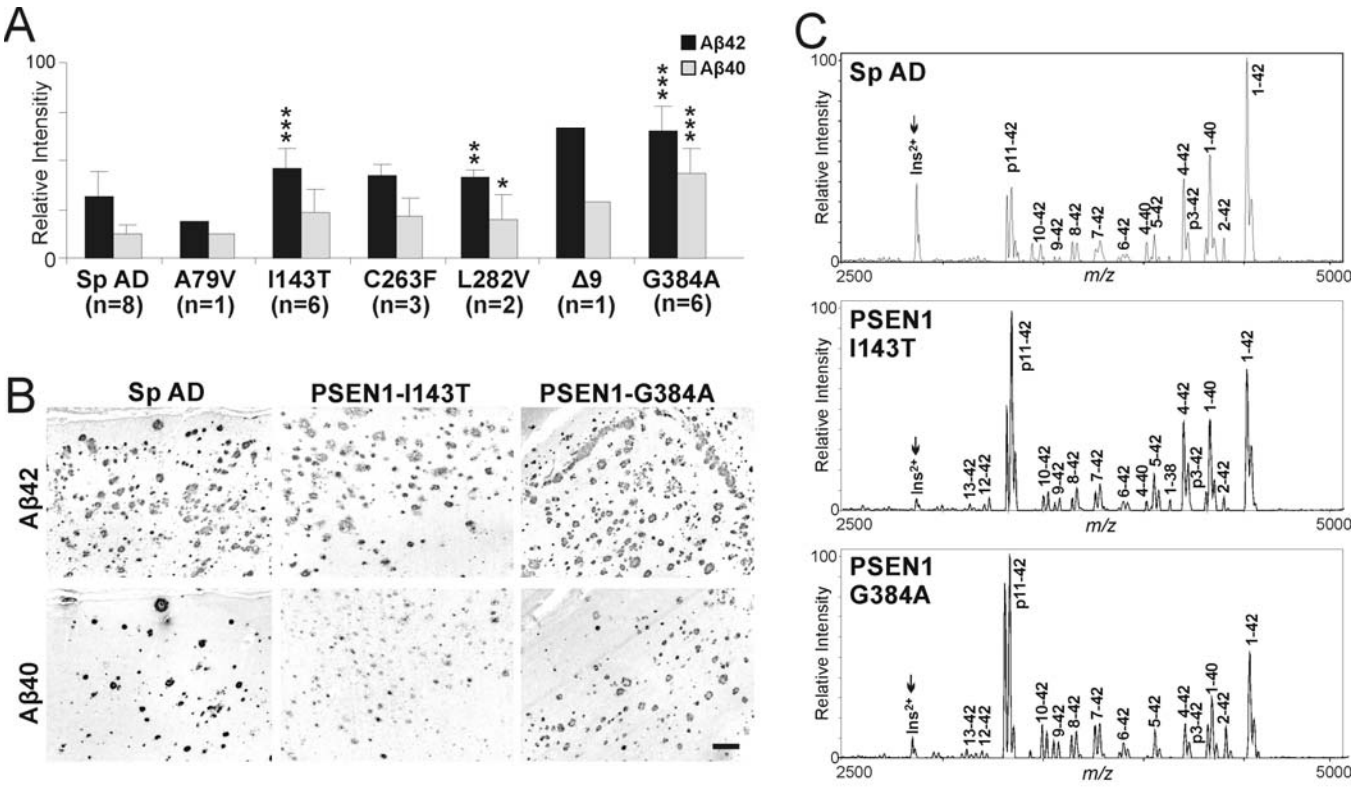
A
Aβ42
Aβ40
Relative Intensity
100
0
***
**
*
***
**
Sp AD (n=8)
A79V (n=1)
I143T (n=6)
C263F (n=3)
L282V (n=2)
Δ9 (n=1)
G384A (n=6)
B
Sp AD
PSEN1-I143T
PSEN1-G384A
Aβ42
Aβ40
C
Sp AD
PSEN1 I143T
PSEN1 G384A
Relative Intensity
m/z
2500
5000
Ins2+
p11-42
1-42
4-42
1-40
2-42
p3-42
10-42
9-42
8-42
7-42
6-42
4-40
5-42
1-38
13-42
12-42

Figure 4